Supporting Information

Designing Multidimensional Hydration Inhibitor towards Long Cycling Performance of Zinc Powder Anode

Chuheng Cao,[a] Wencheng Du,[*b] Cheng Chao Li,[*a] Minghui Ye,[a] Yufei Zhang,[a] Yongchao Tang,[a] Xiaoqing Liu[a]

[a] Guangdong Provincial Key Laboratory of Plant Resources Biorefinery, School of Chemical Engineering and Light Industry, Guangdong University of Technology, Guangzhou 510006, P. R. China

[b] School of Advanced Manufacturing, Guangdong University of Technology, Jieyang 522000, P. R. China

AUTHOR INFORMATION

Corresponding Author

*E-mail:

licc@gdut.edu.cn

duwencheng@gdut.edu.cn

Experimental section

Chemicals: graphite (325 mesh, Aladdin, 99.95 %), sodium citrate dihydrate (Aladdin, 99 %), Zn powder (Shanghai Tianxiang Nanomaterials Co., Ltd.), $ZnSO_4 \cdot 7H_2O$ (Aladdin, 99.9 %), 1-Vinylimidazole (Macklin, 99%), bromoacetic acid (Aladdin, 98%), acetone (Aladdin), diethyl ether (DAMAO), ethanol (Aladdin), 1-Methyl-2-pyrrolidinone (NMP, Aladdin, 99.9 %), polyvinylidene fluoride (PVDF, Aladdin), deionized water.

Preparation of PG: PG was made by organic salt-assisted ultrasonic nondestructive exfoliation of graphite under organic solvents as previously reported.[1, 2] It is generally done by mixing 3 g of natural graphite and 9 g of sodium citrate with 100 mL of ethanol, and then sonicating the solid/liquid mixture for 3 h. The sonicated mixture was placed overnight, then the upper liquid layer was gathered, vacuum filtered, and washed with deionized water to obtain a PG filter cake.

Preparation of Zn powder/PG: To prepare Zn powder/PG, 180 mg of Zn powder and 30 mg of PG were added to a mortar and ground and mixed well. Then the mixture was transferred to a 3 ml slurry bottle, and 300μL NMP was added and stirred overnight to obtain a viscous mixture. The mixture was coated on a copper mesh (12 mm diameter) and dried overnight in a vacuum oven at 80°C. Finally, the dried zinc powder/PG on the copper mesh was pressurized at 10 MPa to obtain a usable zinc powder/PG electrode slice. The mass loading of Zn powder in anodes was about $7 \sim 8$ mg cm^{-2}.

Preparation of CAVImBr: 1-Vinylimidazole (10.0 g, 0.106 mol) and bromoacetic acid (14.7 g, 0.106 mol) were added to 70.0 mL of acetone as a mixture in a 100 mL flask. The mixture was stirred at room temperature for 24 h. The mixture was filtered off, washed with diethyl ether, and finally dried under vacuum at room temperature.

Preparation of rGO hydrogel: rGO hydrogel is obtained via the hydrothermal method.[3] A series of 0.5 mL of graphene oxide dispersion (4.0 mg mL^{-1}) was added in bottle glass (3mL in

size) and then sealed in a 25 mL Teflon lined stainless steel autoclave and then thermal treatment at 180 °C for 2.5 h. After cooling naturally, the product was washed with water.

Preparation of $NH_4V_4O_{10}$: 1.170 g of NH_4VO_3 was dissolved in 40 mL of 80 °C deionized water to form a light yellow solution. After that, 1.891 g of $H_2C_2O_4 \cdot 2H_2O$ solid powder was added to the solution under magnetic stirring until it turned blackish green. The solution was transferred to a 50 ml autoclave and kept in an oven at 140 °C for 48 hours. After natural cooling of the sample to room temperature, the product was collected and washed repeatedly with deionized water. The final product was dried at 60 °C for 12 h to obtain $NH_4V_4O_{10}$.

Preparation of electrolytes: The electrolytes were prepared by mixing 2M $ZnSO_4$ with 1.20M, 1.25M, 1.30M CAVImBr and deionized water in the air. The dosages of electrolyte in a coin cell are 120 μL.

Characterizations:

The morphology characterizations were measured by electron microscope (SEM, Hitachi S-3400N, Japan). XRD patterns were carried out by Rigaku MiniFlex600 powder X-ray diffractometer with Cu Kα radiation (PXRD, Rigaku MiniFlex600, Japan). The Raman spectra were obtained by using a Raman spectrometer (LabRAM HR Evolution, France). The ionic conductivity of electrolytes was measured by a Conductivity meter (DDS-308A, China). The contact angle of electrolytes was measured by the Contact Angle Analyzer (OCA100, Germany). AFM height images were measured by Scanning Probe Microscope (Dimension FastScan, USA). ^{1}H-NMR spectrum was measured by Superconducting Fourier nuclear magnetic resonance apparatus (AVANCE III 400 MHz, SH). The X-ray photoelectron spectroscopy (XPS) analysis was carried out by Escalab 250 Xi X-ray photoelectron spectrometer (Thermo Fisher).

Electrochemical measurements:

The electrochemical performances of Zn powder/PG composites were evaluated with a CR2032 coin cell. Glass fiber filter paper (675μm, Whatman GF/D) was used as the separator. The galvanostatic plating/stripping curves of Zn were performed on a NEWARE battery testing system conducted at different current densities with a series of areal capacities. Tafel plots were measured in the three-electrode electrochemical cell on Gamry electrochemical workstation. Liner sweep voltammetry (LSV) and cyclic voltammetry (CV) were assembled into coin cells for testing on Gamry electrochemical workstation with a scanning rate of 1mV s^{-1}. Electrochemical impedance spectroscopy (EIS) measurements are recorded on an electrochemical workstation in the frequency range from 100 kHz to 0.01Hz.

For $NH_4V_4O_{10}$||Zn powder/PG full cells, to prepare the $NH_4V_4O_{10}$ cathode, the $NH_4V_4O_{10}$, carbon black and PVDF binder were mixed in a weight ratio of 7:2:1 with NMP as solvent to form a homogeneous slurry. This slurry was then uniformly spread onto carbon paper, and then dried at 80°C in a vacuum oven for a whole night. The mass loading of active material in cathodes was about 3~4 mg cm^{-2}. The coin cells were assembled in the atmosphere at room temperature. The cells were galvanostatically charged and discharged between 0.3 and 1.3 V versus Zn^{2+}/Zn on a Neware battery tester. The specific capacities were calculated based on the mass of $NH_4V_4O_{10}$.

For PANI||Zn powder/PG full cells, the commercial PANI, carbon black and PVDF binder were mixed in a weight ratio of 5:4:1 with NMP as solvent to form a homogeneous slurry. This slurry was then uniformly spread onto carbon paper, and then dried at 80°C in a vacuum oven for a whole night. The mass loading of active material in cathodes was about 1~2 mg cm^{-2}. The coin cells were assembled in the atmosphere at room temperature and filter paper was used as a separator. The cells were galvanostatically charged and discharged between 0.5 and 1.6 V versus Zn^{2+}/Zn on a Neware battery tester. The specific capacities were calculated based on the mass of PANI.

Electrochemical performances of Zinc-ion capacitors (ZICs) were tested using two-electrode cells. Assembly of the two-electrode cells was similar to the reported method for the capacitor (**Scheme S1**).[4, 5] Zn powder/PG as negative electrodes, and rGO-loaded carbon paper with 1 mg solid materials served as positive electrodes. Filter paper as the separator, and 107 μL electrolyte was used. Galvanostatic charging/discharging (GCD), and open circuit potential-time curve were performed by an electrochemical workstation (DyneChem).
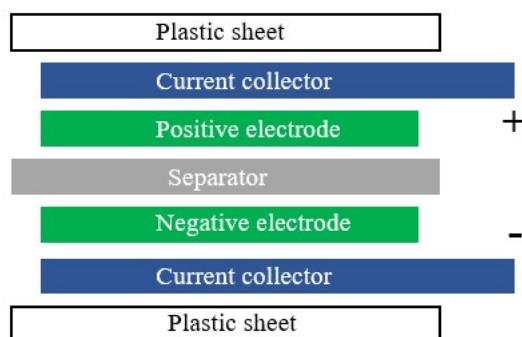
Scheme S1 Schematic illustration of a ZIC cell

The specific gravimetric capacitance (C_g, F g^{-1}) of rGO was calculated using GCD curves by the following formula:

$$C_g = I \times \Delta t / (m \times \Delta U)$$

where I is the current density, Δt is the discharging time, m is the mass loading of rGO, and ΔU is the voltage difference of the discharge curve.

Theoretical computational details

The binding energy calculations were performed using the Gaussian 16 package. And the structures of the molecules were optimized at the B3LYP/6-311G(d) level for H, O, and Br elements and B3LYP/SDD level for Zn. The binding energy (Eb) between Zn ions and H_2O solvent or Br ions is defined as follows:

$$E_b = E_{complex} - E_{cation} - E_{solvent/anion}$$

where $E_{complex}$ is the total energy of cation-solvent/anion complex, E_{cation} is the energy of a cation, $E_{solvent/anion}$ is the energy of a solvent or anion.

The adsorption energies in this work were performed in the framework of the density functional theory (DFT) with the projector augmented plane-wave method, as implemented in the Vienna ab initio simulation package (VASP).[6, 7] The generalized gradient approximation proposed by Perdew-Burke-Ernzerhof (PBE), is selected for the exchange-correlation potential.[8] The cut-off energy for a plane wave is set to 400 eV. The energy criterion is set to 10^{-4} eV in the iterative solution of the Kohn-Sham equation. All the structures are relaxed until the residual forces on the atoms have declined to less than 0.02 eV/Å. The adsorbed energy between the Zn slab and H_2O/CAVIm$^+$ solvent or Br ions were defined as the following equation:

$$E_{ad} = E_{Zn-slab+solvent/anion} - E_{Zn-slab} - E_{solvent/anion}$$

Where $E_{Zn-slab+solvent/anion}$ is the total energy of Zn-slab with absorbed solvent or anion, $E_{Zn-slab}$ is the energy of a free Zn-slab, $E_{solvent}$ is the energy of a solvent.
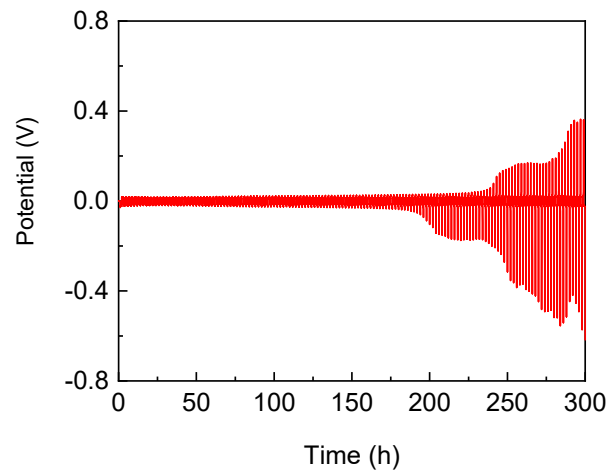
Figure S1 Severe polarization of Zn powder/PG electrodes symmetric cells in ZnSO$_4$ electrolyte at 1mA cm^{-2} with a capacity of 1mAh cm^{-2}.
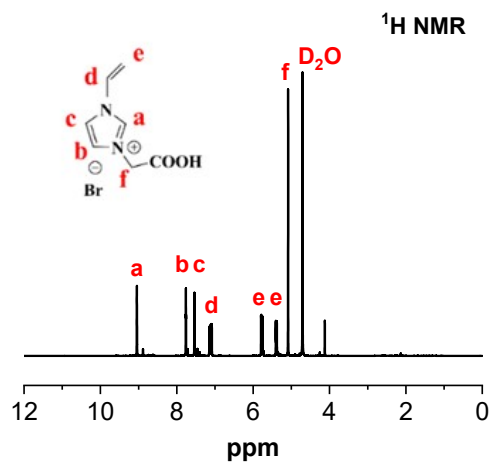
Figure S2 ¹H-NMR spectrum of 1-carboxymethyl-3-vinylimidazolium bromide.
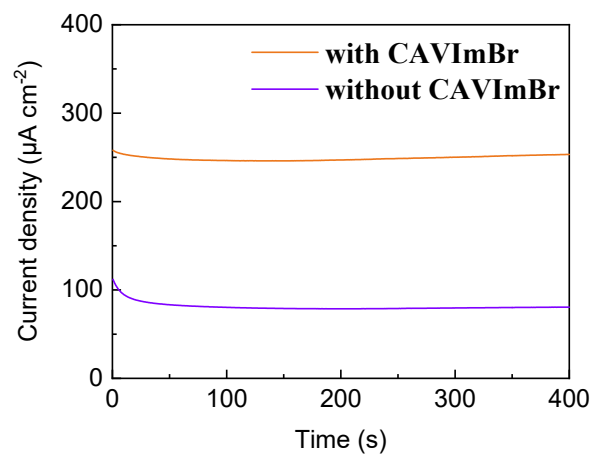
Figure S3 The Chronoamperograms of Zn powder/PG symmetric cells in $ZnSO_4$ electrolyte with and without CAVImBr at 10 mV.
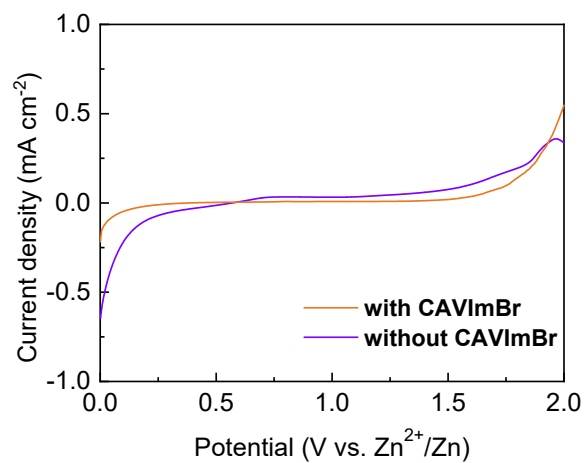
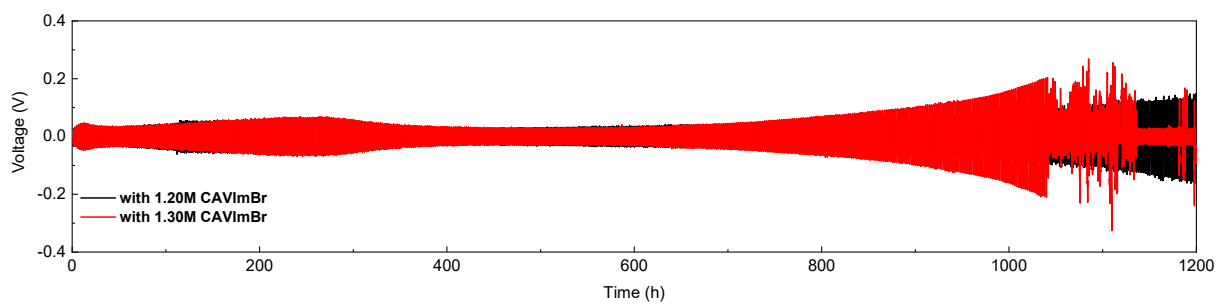**Figure S4** Electrochemical windows of ZnSO$_4$ electrolyte with and without CAVImBr.

Figure S5 Cycling performance of Zn powder/PG electrodes symmetric cells in ZnSO$_4$ electrolyte with 1.20M and 1.30 M CAVImBr at 1mA cm^{-2} with a capacity of 1mAh cm^{-2}.
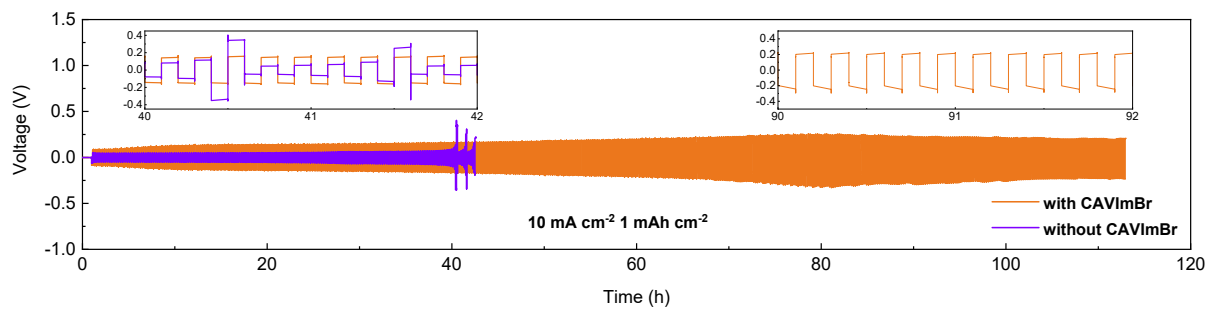
Figure S6 Cycling performance of Zn powder/PG electrodes symmetric cells in ZnSO$_4$ electrolyte with and without CAVImBr at 10 mA cm^{-2} with a capacity of 1 mAh cm^{-2}.
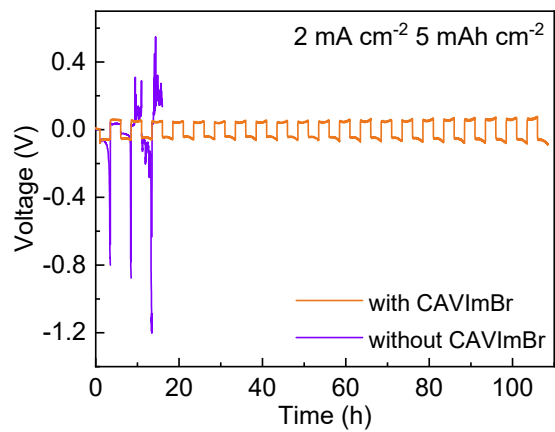
Figure S7 Cycling performance of Zn powder/PG electrodes symmetric cells in $ZnSO_4$ electrolyte with and without CAVImBr at 2 mA cm^{-2} with a capacity of 5 mAh cm^{-2} (DOD=86%).
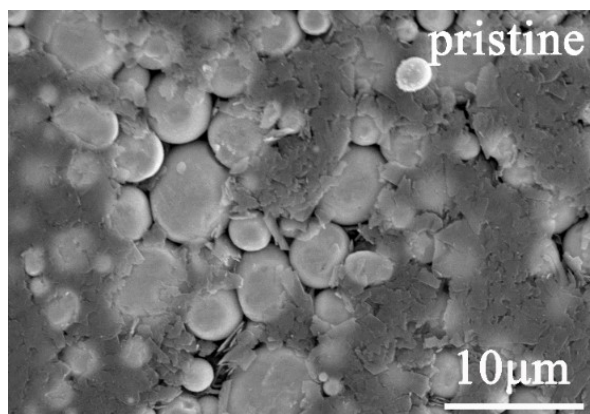
Figure S8 Top view SEM images of pristine Zn powder/PG electrodes.
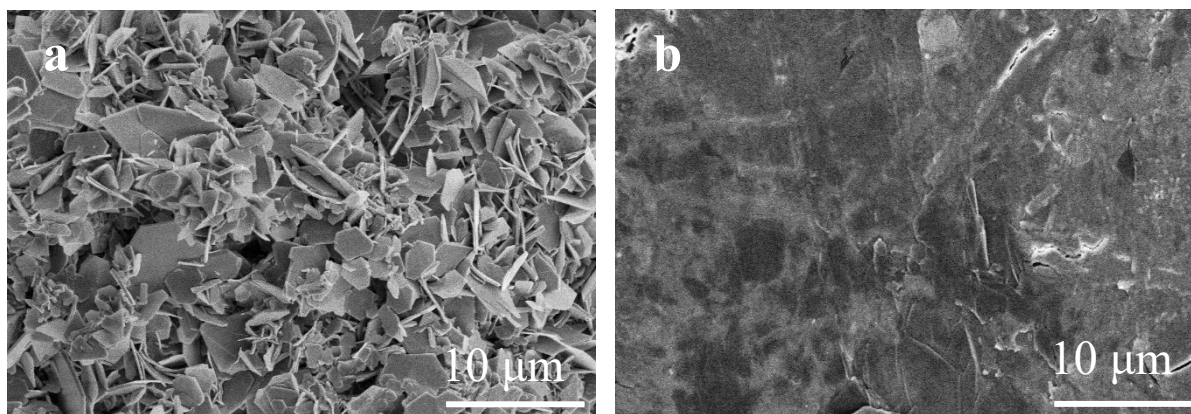
Figure S9 Top view SEM images of Zn powder/PG electrodes symmetrical cells after 20 cycles in ZnSO$_4$ electrolyte (a) without CAVImBr and (b) with CAVImBr (3 mA cm^{-2}, 3 mAh cm^{-2}).
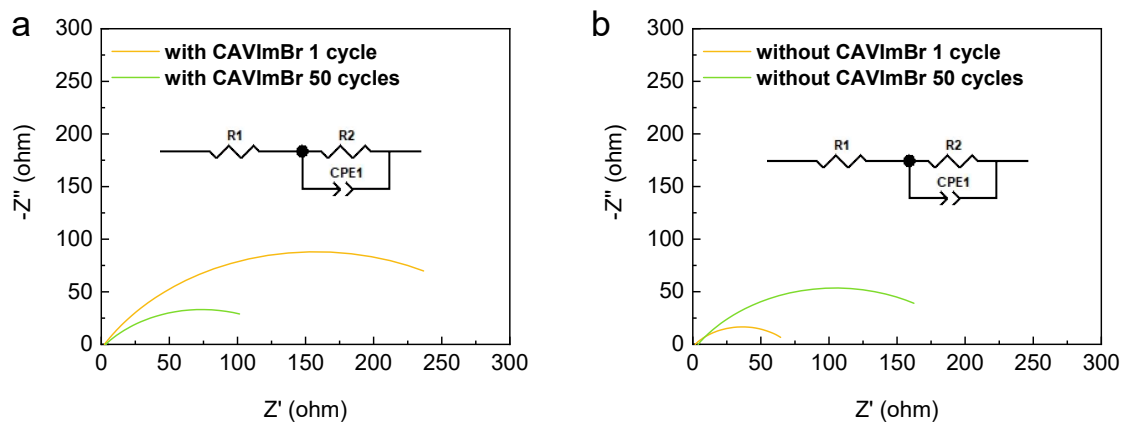
Figure S10 Nyquist plots of Zn powder/PG electrodes symmetrical cells after 1 and 50 cycles in ZnSO$_4$ electrolyte (a) with CAVImBr and (b) without CAVImBr (1 mA cm^{-2}, 1 mAh cm^{-2}). The inset is the equivalent circuit of EIS.
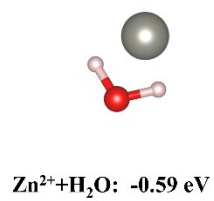
Zn²⁺+H₂O: -0.59 eV **Zn²⁺+Br⁻: -1.78 eV**
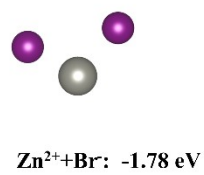
Figure S11 The binding energy of Zn^{2+} with H_2O molecules and Br^-.
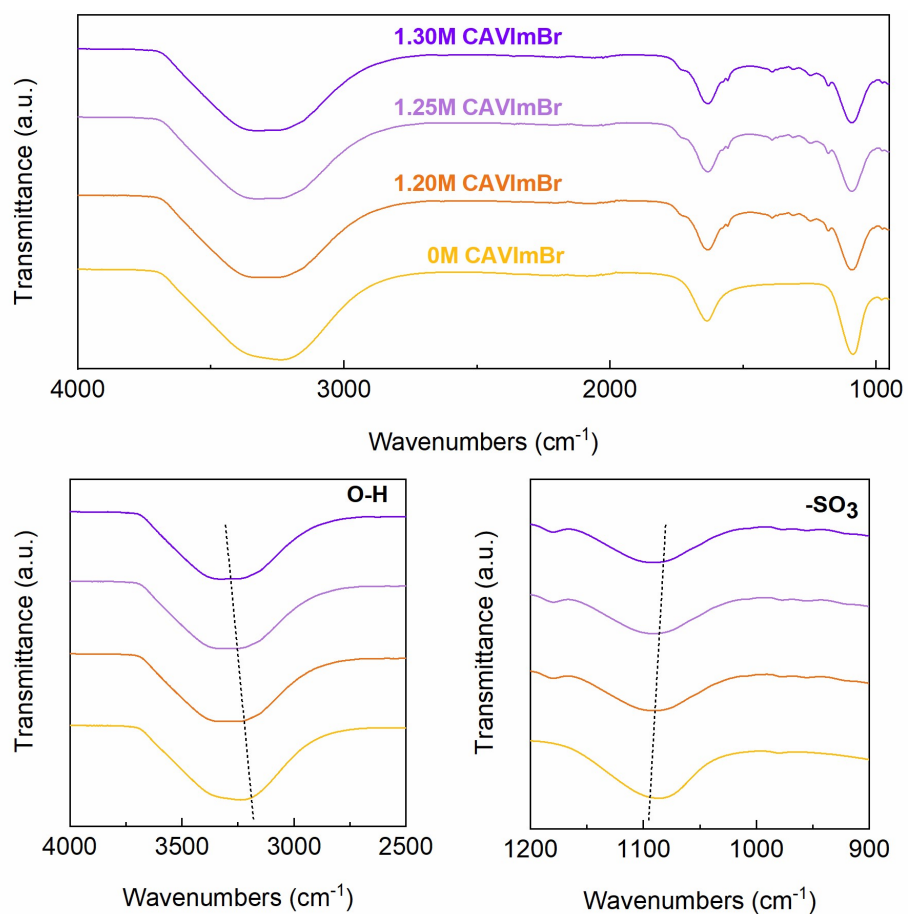
Figure S12 FTIR spectra of O-H (a) and -SO_4^{2-} (b) stretching vibration range with different concentrations of CAVImBr added in the 2M $ZnSO_4$ electrolytes.
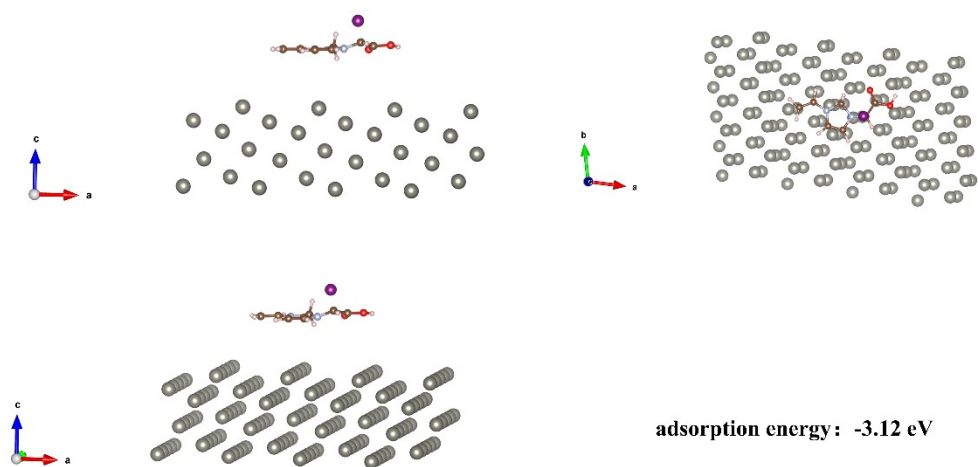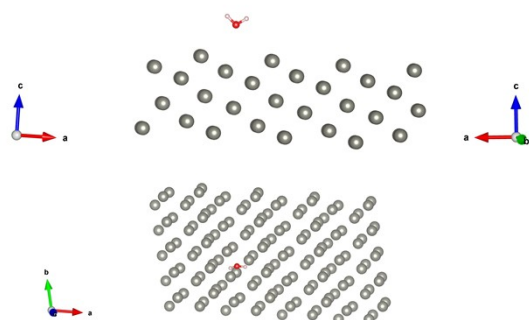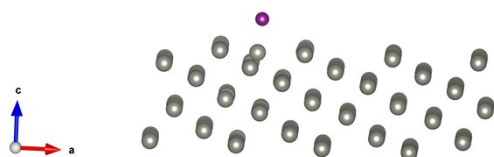
Zn (101) – CAVIm⁺

adsorption energy：-3.12 eV

Figure S13 The adsorption energy of CAVIm⁺ on the Zn (101) plane.

Zn (101) – H₂O

adsorption energy：-0.11 eV

Zn (101) – Br⁻

adsorption energy：-0.97 eV

Figure S14 The adsorption energy of H₂O molecules and Br⁻ on the Zn (101) plane.

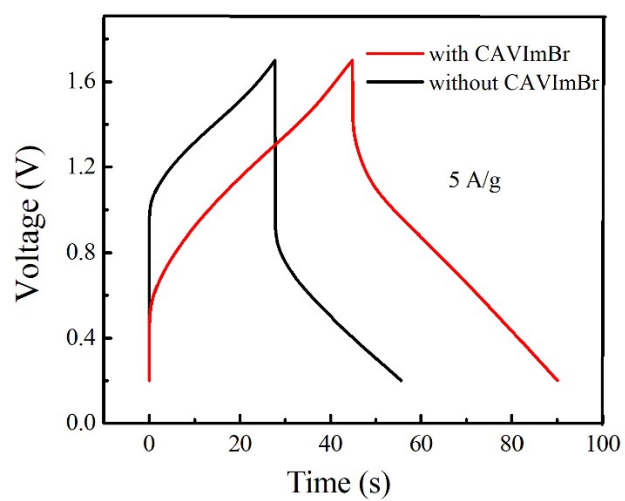**Figure S15** The digital image of rGO hydrogel prepared by hydrothermal method.

Figure S16 GCD curves at the current density of 5A g^{-1} for ZIC devices in $ZnSO_4$ electrolyte with and without CAVImBr.
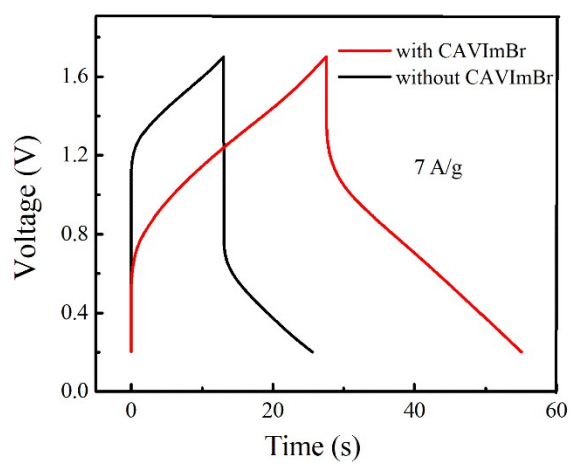
Figure S17 GCD curves at the current density of 7 A g^{-1} for ZIC devices in ZnSO$_4$ electrolyte with and without CAVImBr.
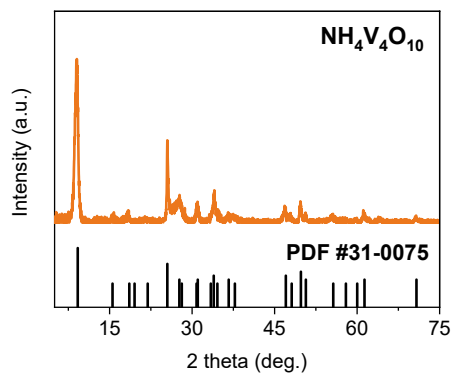
.

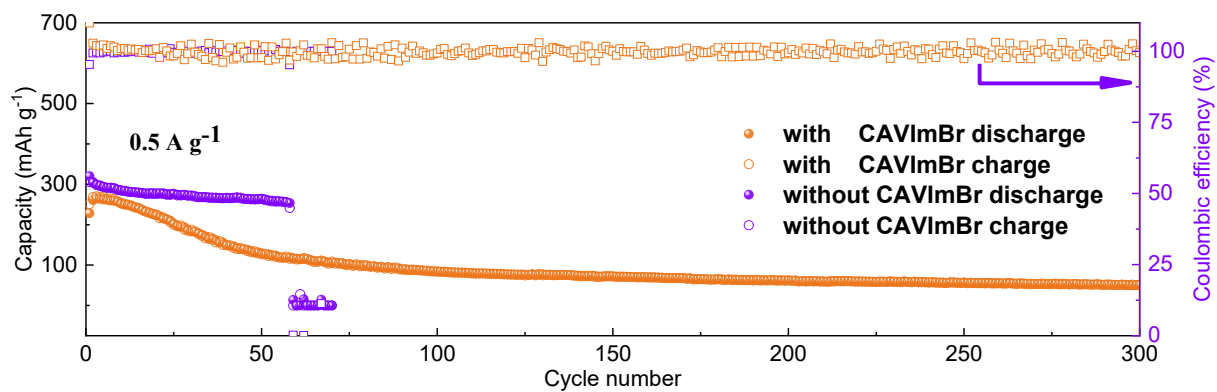**Figure S18** XRD pattern of the as-prepared $NH_4V_4O_{10}$.

Figure S19 Comparison of cycling performances of $NH_4V_4O_{10}\|Zn$ powder/PG full cells with and without CAVImBr added in the 2M $ZnSO_4$ electrolytes at a rate of 0.5 A g^{-1}.

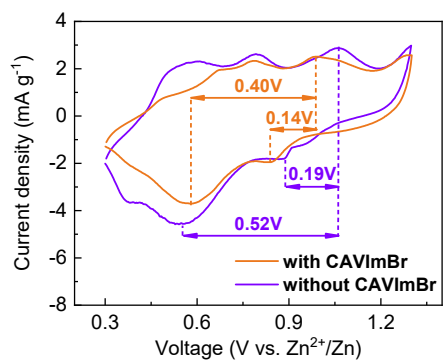**Figure S20** The CV curves of $NH_4V_4O_{10}$||Zn powder/PG full cells with and without CAVImBr added in the 2M $ZnSO_4$ electrolytes.
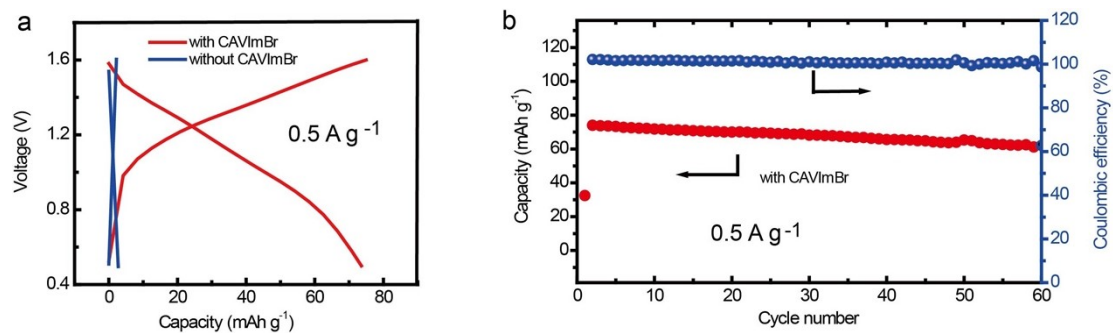
Figure S21 (a) Galvanostatic charge/discharge curves of PANI∥Zn powder/PG batteries with and without CAVImBr added in the 2M $ZnSO_4$ electrolytes at a rate of 0.5 A g^{-1}, and (b) corresponding cycling performance of PANI∥Zn powder/PG full cell.

Table S1 Comparison of electrochemical performances of this work with previously reported symmetric Zn-based cells.

Zn-based anodes	Electrolyte	Current density, Capacity ($mA\ cm^{-2}$, $mAh\ cm^{-2}$)	Lifespan (hour)	DOD (%)	Ref.
Ti_3C_2Tx MXene@Zn Powder	2 M $ZnSO_4$	1-0.5	200	-	[9]
Zn powder/PG	2 M $ZnSO_4$	1-1 5-0.5	400 360	15	[10]
Zn-P-MIEC	2 M $ZnSO_4$	0.25-0.05 1-1 2-2 5-2 10-1	1270 400 220 180 100	-	[11]
Zn powder	1 M $Zn(TFSI)_2$ + 20 M LiTFSI	0.2-0.068	170	-	[12]
Zn foil	30 mol.% H2O in a eutectic mixture of urea/LiTFSI/$Zn(TFSI)_2$	0.02-0.2	450	~1.8	[13]
Zn plate	0.5 M $Zn(CF_3SO_3)_2$ in triethyl phosphate: H_2O (7:3)	1-1	200	~0.7	[14]
Zn powder/PG	2 M $ZnSO_4$+ 1.25 M CAVImBr	1-1 5-1 10-1	1100 245 115	17	This work

References

1   W. Du, J. Lu, P. Sun, Y. Zhu and X. Jiang, *Chem. Phys. Lett.*, 2013, **568-569**, 198-201.
2   W. Du, S. Qi, Y. Zhu, P. Sun, L. Zhu and X. Jiang, *Chem. Eng. J.*, 2015, **262**, 658-664.
3   Yuxi Xu, Kaixuan Sheng, Chun Li and G. Shi, *ACS Nano*, 2010, **4**, 4324–4330.
4   Meryl D. Stoller, Sungjin Park, Yanwu Zhu, Jinho An and R. S. Ruoff, *Nano Lett.*, 2008, **8**, 3498–3502.
5   Qiong Wu, Yuxi Xu, Zhiyi Yao, Anran Liu and G. Shi, *ACS Nano*, 2010, **4**, 1963–1970.
6   John P. Perdew, Kieron Burke and M. Ernzerhof, *Phys. Rev. Lett.*, 1996, **77**, 3865-3868.
7   G. Kresse and J. Furthmüller, *Phy. Rev. B*, 1996, **54**, 11169-11186.
8   R. Xiao, H. Li and L. Chen, *Sci. Rep.*, 2015, **5**, 14227.
9   X. Li, Q. Li, Y. Hou, Q. Yang, Z. Chen, Z. Huang, G. Liang, Y. Zhao, L. Ma, M. Li, Q. Huang and C. Zhi, *ACS Nano*, 2021, **15**, 14631-14642.
10 W. Du, S. Huang, Y. Zhang, M. Ye and C. C. Li, *Energy Storage Mater.*, 2022, **45**, 465-473.
11 M. Zhang, P. Yu, K. Xiong, Y. Wang, Y. Liu and Y. Liang, *Adv.Mater.*, 2022, **34**, 2200860.
12 F. Wang, O. Borodin, T. Gao, X. Fan, W. Sun, F. Han, A. Faraone, J. A. Dura, K. Xu and C. Wang, *Nat. Mater.*, 2018, **17**, 543-549.
13 J. Zhao, J. Zhang, W. Yang, B. Chen, Z. Zhao, H. Qiu, S. Dong, X. Zhou, G. Cui and L. Chen, *Nano Energy*, 2019, **57**, 625-634.
14 A. Naveed, H. Yang, J. Yang, Y. Nuli and J. Wang, *Angew. Chem. Int. Ed.*, 2019, **58**, 2760-2764.